Supplemental Material for *Optimizing allocation for a delayed influenza vaccination campaign*

Jan Medlock*† Lauren A. Meyers‡§ Alison P. Galvani¶

November 19, 2009

We extended the age-structured SEIR (susceptible, latent, infectious, recovered) model of Medlock and Galvani [6] to include two levels of risk for complications due to influenza infection and parametrized this model using data from the 2009 H1N1 influenza pandemic. We also extended the framework to incorporate staggered delivery of vaccine doses.

Here we detail the model construction and parametrization and review the results.

S1 Mathematical Model

S1.1 Transmission Model

For modeling influenza transmission in the United States, we divide the population into the 17 age groups for ages 0, 1–4, 5–9, 10–14, 15–19, 20–24, 25–29, 30–34, 35–39, 40–44, 45–49, 50–54, 55–59, 60–64, 65–69, 70–74, and 75+. The numbers of people in each age group were parametrized using the estimated US 2007 population [17].

*Department of Mathematical Sciences, Clemson University, Box 340975, Clemson, SC 29634

†Corresponding author. Email: medlock@clemson.edu

‡Section of Integrative Biology, The University of Texas at Austin, Austin, TX 78712

§Santa Fe Institute, 1399 Hyde Park Road, Santa Fe, NM 87501

¶Department of Epidemiology and Public Health, Yale University School of Medicine, 135 College Street, New Haven, CT 06520

Within each age, we further divide the population into low risk and high risk for influenza complications, with high risk being identified by existing medical conditions such as asthma, heart disease, and pregnancy. The proportion high risk by age is given in Table S1 [8]. (Where the age groups for the proportion at high risk do not line up with our model age groups, we assumed that people are distributed uniformly within the model age groups. E.g. we assume that from the age group 15–19, 80% are under 18 and 20% are over 18.)

Each of the age–risk groups is then stratified by infection status. Let $S_{\mathrm{LU}a}(t)$, $E_{\mathrm{LU}a}(t)$, $I_{\mathrm{LU}a}(t)$, and $R_{\mathrm{LU}a}(t)$ be the respective numbers of unvaccinated low-risk susceptible, latent, infectious, and recovered people in age groups $a = 1, 2, \ldots, 17$. Let $S_{\mathrm{HU}a}(t)$, $E_{\mathrm{HU}a}(t)$, $I_{\mathrm{HU}a}(t)$, and $R_{\mathrm{HU}a}(t)$ be defined similarly, but for unvaccinated high-risk people. Now, let $S_{\mathrm{LV}a}(t)$, $E_{\mathrm{LV}a}(t)$, $I_{\mathrm{LV}a}(t)$, $R_{\mathrm{LV}a}(t)$, $S_{\mathrm{HV}a}(t)$, $E_{\mathrm{HV}a}(t)$, $I_{\mathrm{HV}a}(t)$, $R_{\mathrm{HV}a}(t)$ be defined similarly for vaccinated people.

Table S1: Proprtion at high risk for influenza complications.

Ages	**Proportion High Risk,** $P_{\mathrm{H}a}$
$<$ 6 m	1.51%
6 m–1	4.22%
1–4	8.86%
5–18	11.92%
19–24	18.79%
25–49	20.15%
50–64	33.83%
65+	53.15%

Compiled by the MIDAS High-Risk Segmentation Group [8]. High risk for influenza complications is defined as having a chronic condition that is indications receiving influenza vaccine, having an immunocompromised condition, or being pregnant. For adults, the chronic conditions that indicate vaccination are: current asthma, chronic bronchitis, emphysema, coronary heart disease, angina, heart attack, diabetes, stroke, weak kidney, epilepsy, cerebral palsy, movement disorders, and muscular dystrophies [2]. For children, these chronic conditions are: current asthma, congenital heart disease, ever diabetes, Down syndrome, ever cerebral palsy, ever muscular dystrophy, ever cystic fibrosis, ever sickle cell anemia, and seizures in past 12 months [2]. For children under 6 months, birth weight less than 1500 gm is also included [2]. Immunocompromised conditions are: cancer in the past 3 years [2], HIV/AIDS [3], dialysis [16], and having had an organ transplant [11]. Pregnancy is also included [2].

The infection dynamics are described by the differential equations

$$\frac{\mathrm{d}S_{\mathrm{LU}a}}{\mathrm{d}t} = -\lambda_a S_{\mathrm{LU}a}, \tag{S1a}$$
$$\frac{\mathrm{d}E_{\mathrm{LU}a}}{\mathrm{d}t} = \lambda_a S_{\mathrm{LU}a} - \tau E_{\mathrm{LU}a}, \tag{S1b}$$
$$\frac{\mathrm{d}I_{\mathrm{LU}a}}{\mathrm{d}t} = \tau E_{\mathrm{LU}a} - (\gamma + \nu_{\mathrm{LU}a}) I_{\mathrm{LU}a}, \tag{S1c}$$
$$\frac{\mathrm{d}R_{\mathrm{LU}a}}{\mathrm{d}t} = \gamma I_{\mathrm{LU}a}, \tag{S1d}$$
$$\frac{\mathrm{d}S_{\mathrm{HU}a}}{\mathrm{d}t} = -\lambda_a S_{\mathrm{HU}a}, \tag{S1e}$$
$$\frac{\mathrm{d}E_{\mathrm{HU}a}}{\mathrm{d}t} = \lambda_a S_{\mathrm{HU}a} - \tau E_{\mathrm{HU}a}, \tag{S1f}$$
$$\frac{\mathrm{d}I_{\mathrm{HU}a}}{\mathrm{d}t} = \tau E_{\mathrm{HU}a} - (\gamma + \nu_{\mathrm{HU}a}) I_{\mathrm{HU}a}, \tag{S1g}$$
$$\frac{\mathrm{d}R_{\mathrm{HU}a}}{\mathrm{d}t} = \gamma I_{\mathrm{HU}a}, \tag{S1h}$$
$$\frac{\mathrm{d}S_{\mathrm{LV}a}}{\mathrm{d}t} = -(1-\epsilon_a)\lambda_a S_{\mathrm{LV}a}, \tag{S1i}$$
$$\frac{\mathrm{d}E_{\mathrm{LV}a}}{\mathrm{d}t} = (1-\epsilon_a)\lambda_a S_{\mathrm{LV}a} - \tau E_{\mathrm{LV}a}, \tag{S1j}$$
$$\frac{\mathrm{d}I_{\mathrm{LV}a}}{\mathrm{d}t} = \tau E_{\mathrm{LV}a} - (\gamma + \nu_{\mathrm{LV}a}) I_{\mathrm{LV}a}, \tag{S1k}$$
$$\frac{\mathrm{d}R_{\mathrm{LV}a}}{\mathrm{d}t} = \gamma I_{\mathrm{LV}a}, \tag{S1l}$$
$$\frac{\mathrm{d}S_{\mathrm{HV}a}}{\mathrm{d}t} = -(1-\epsilon_a)\lambda_a S_{\mathrm{HV}a}, \tag{S1m}$$
$$\frac{\mathrm{d}E_{\mathrm{HV}a}}{\mathrm{d}t} = (1-\epsilon_a)\lambda_a S_{\mathrm{HV}a} - \tau E_{\mathrm{HV}a}, \tag{S1n}$$
$$\frac{\mathrm{d}I_{\mathrm{HV}a}}{\mathrm{d}t} = \tau E_{\mathrm{HV}a} - (\gamma + \nu_{\mathrm{HV}a}) I_{\mathrm{HV}a}, \tag{S1o}$$
$$\frac{\mathrm{d}R_{\mathrm{HV}a}}{\mathrm{d}t} = \gamma I_{\mathrm{HV}a} \tag{S1p}$$

for $a = 1, \ldots, 17$. The progression rate to infectiousness is τ and the recovery rate is γ. The influenza-induced death rates for people in age group a are $\nu_{\mathrm{LU}a}$, $\nu_{\mathrm{HU}a}$, $\nu_{\mathrm{LV}a}$, and $\nu_{\mathrm{HV}a}$, respectively, for unvaccinated low-risk, unvaccinated high-risk, vaccinated low-risk, and vaccinated high-risk people. The

force of infection is given by

$$\begin{aligned}\lambda_a &= \sum_{\alpha=1}^{17} \frac{\beta\sigma_a\phi_{a\alpha}\left(I_{\mathrm{LU}\alpha} + I_{\mathrm{HU}\alpha} + I_{\mathrm{LV}\alpha} + I_{\mathrm{HV}\alpha}\right)}{N} \\ &= \frac{\beta\sigma_a}{N}\sum_{\alpha=1}^{17}\phi_{a\alpha}\left(I_{\mathrm{LU}\alpha} + I_{\mathrm{HU}\alpha} + I_{\mathrm{LV}\alpha} + I_{\mathrm{HV}\alpha}\right).\end{aligned} \tag{S1q}$$

Here $\phi_{a\alpha}$ is the number of contacts between a person in age group a with people in age group α, β is the probability of infection for a susceptible person who has contact with an infectious person, and σ_a is the relative susceptibility of people in age group a. The relative susceptibility incorporates the potential for older people to have some immunity to the current 2009 H1N1 strain due to exposure to a similar virus in the distant past. The total population size is N:

$$\begin{aligned}N_a = {} & S_{\mathrm{LU}a} + E_{\mathrm{LU}a} + I_{\mathrm{LU}a} + R_{\mathrm{LU}a} + S_{\mathrm{HU}a} + E_{\mathrm{HU}a} + I_{\mathrm{HU}a} + R_{\mathrm{HU}a} \\ & + S_{\mathrm{LV}a} + E_{\mathrm{LV}a} + I_{\mathrm{LV}a} + R_{\mathrm{LV}a} + S_{\mathrm{HV}a} + E_{\mathrm{HV}a} + I_{\mathrm{HV}a} + R_{\mathrm{HV}a},\end{aligned} \tag{S1r}$$

$$N = \sum_a N_a. \tag{S1s}$$

The demographic effects of aging, birth, and death by causes not related to influenza are not included because we only model one influenza season, where these demographic effects are small.

The epidemic is initiated with the entire population unvaccinated, with one person of each age infectious, and the remaining population susceptible.

That is

$$S_{\mathrm{LU}a}(t_0) = (1 - P_{\mathrm{H}a})N_a - 1, \tag{S2a}$$
$$S_{\mathrm{HU}a}(t_0) = P_{\mathrm{H}a}N_a - 1, \tag{S2b}$$
$$S_{\mathrm{LV}a}(t_0) = 0, \tag{S2c}$$
$$S_{\mathrm{HV}a}(t_0) = 0, \tag{S2d}$$
$$E_{\mathrm{LU}a}(t_0) = 0, \tag{S2e}$$
$$E_{\mathrm{HU}a}(t_0) = 0, \tag{S2f}$$
$$E_{\mathrm{LV}a}(t_0) = 0, \tag{S2g}$$
$$E_{\mathrm{HV}a}(t_0) = 0, \tag{S2h}$$
$$I_{\mathrm{LU}a}(t_0) = 1, \tag{S2i}$$
$$I_{\mathrm{HU}a}(t_0) = 1, \tag{S2j}$$
$$I_{\mathrm{LV}a}(t_0) = 0, \tag{S2k}$$
$$I_{\mathrm{HV}a}(t_0) = 0, \tag{S2l}$$
$$R_{\mathrm{LU}a}(t_0) = 0, \tag{S2m}$$
$$R_{\mathrm{HU}a}(t_0) = 0, \tag{S2n}$$
$$R_{\mathrm{LV}a}(t_0) = 0, \tag{S2o}$$
$$R_{\mathrm{HV}a}(t_0) = 0, \tag{S2p}$$

where N_a is the number of people of age a (from the estimated 2007 US population [17]) and $P_{\mathrm{H}a}$ is the proportion of age group a who are high risk (Table S1).

Numerical solution of the model differential equations was done using the LSODA routine [5].

S1.2 Basic Reproductive Number

The basic reproductive number (R_0) of model (S1) was calculated using the next-generation matrix ([4, 6, 18]). No closed form expression is available for R_0 for model (S1): rather, it is given by the leading eigenvalue of a matrix depending on the model parameters.

Consider the case when no one in the population has been exposed to the

pathogen and there is no vaccination. Define the sub-matrices

$$\mathbf{F}_{\mathrm{L}} = [F_{\mathrm{L}a\alpha}] = \left[\beta\sigma_a \frac{(1-P_{\mathrm{H}a})N_a}{N}\phi_{a\alpha}\right], \tag{S3a}$$

$$\mathbf{F}_{\mathrm{H}} = [F_{\mathrm{H}a\alpha}] = \left[\beta\sigma_a \frac{P_{\mathrm{H}a}N_a}{N}\phi_{a\alpha}\right], \tag{S3b}$$

$$\mathbf{V}_{\mathrm{L}} = [V_{\mathrm{L}a\alpha}] = [\gamma + \nu_{\mathrm{LU}a}\delta_{a\alpha}], \tag{S3c}$$

$$\mathbf{V}_{\mathrm{H}} = [V_{\mathrm{H}a\alpha}] = [\gamma + \nu_{\mathrm{HU}a}\delta_{a\alpha}]. \tag{S3d}$$

Here, $\delta_{a\alpha}$ is the Dirac delta:

$$\delta_{a\alpha} = \begin{cases} 1, & \text{if } a = \alpha, \\ 0, & \text{otherwise.} \end{cases} \tag{S4}$$

Now define the matrices

$$\mathbf{F} = \begin{bmatrix} \mathbf{F}_{\mathrm{L}} & \mathbf{0} \\ \mathbf{0} & \mathbf{F}_{\mathrm{H}} \end{bmatrix}, \tag{S5a}$$

$$\mathbf{V} = \begin{bmatrix} \mathbf{V}_{\mathrm{L}} & \mathbf{0} \\ \mathbf{0} & \mathbf{V}_{\mathrm{H}} \end{bmatrix}. \tag{S5b}$$

Finally,

$$R_0 = \rho\left(\mathbf{F}\mathbf{V}^{-1}\right), \tag{S6}$$

where $\rho(\mathbf{M})$ is the largest magnitude of the eigenvalues of the matrix $\mathbf{M}$.

This calculation of R_0 is easily extended to include a population with both unvaccinated and vaccinated people.

S1.3 Optimal Vaccine Allocation

A vaccine delivery schedule is a list of amounts of vaccine available (v_r) and the time (in days) at which they are available (t_r), for $r = 1, 2, \ldots, R$, for a total of R batches of vaccine availability. For example, a schedule with 45 million doses available on day t_1 and 20 million doses available each week thereafter for 3 weeks would have $t_1 = t_1, v_1 = 45\,000\,000$, $t_2 = t_1 + 7, v_2 = 20\,000\,000$, $t_3 = t_1 + 14, v_3 = 20\,000\,000$, and $t_4 = t_1 + 21, v_4 = 20\,000\,000$.

Let $p_{\mathrm{L}ra_{\mathrm{L}}}$ be the proportion of the vaccine that is available at time t_r that is given to low-risk people in age group a_{L} and $p_{\mathrm{H}ra_{\mathrm{H}}}$ be the proportion given to high-risk people in age group a_{H}; these are the control variables. New

age groups, $a_{\mathrm{L}} = 1, 2, \ldots, A_{\mathrm{L}}$ and $a_{\mathrm{H}} = 1, 2, \ldots, A_{\mathrm{H}}$ have been introduced to allow for vaccine policies that have different age groups than those in model (S1) itself. In particular, we will consider that we wish to find the best way to distribute vaccine to the 5 low-risk age groups ($A_{\mathrm{L}} = 5$) 0–4, 5–17, 18–44, 45–64, and 65+ and a single group for high-risk people of all ages ($A_{\mathrm{H}} = 1$). The factor $G_{\mathrm{L}aa_{\mathrm{L}}}$ is the fraction of low-risk people in model age group a who are also in vaccination age group a_{L} and $G_{\mathrm{H}aa_{\mathrm{H}}}$ is defined similarly for high-risk people: these convert between the age groups used in model (S1) and those used as the basis for vaccine distribution. For our age groups, these are

$$\mathbf{G}_{\mathrm{L}} = \begin{bmatrix} 1 & 1 & 0 & 0 & 0 & 0 & 0 & 0 & 0 & 0 & 0 & 0 & 0 & 0 & 0 & 0 & 0 \\ 0 & 0 & 1 & 1 & 0.8 & 0 & 0 & 0 & 0 & 0 & 0 & 0 & 0 & 0 & 0 & 0 & 0 \\ 0 & 0 & 0 & 0 & 0.2 & 1 & 1 & 1 & 1 & 1 & 0 & 0 & 0 & 0 & 0 & 0 & 0 \\ 0 & 0 & 0 & 0 & 0 & 0 & 0 & 0 & 0 & 0 & 1 & 1 & 1 & 1 & 0 & 0 & 0 \\ 0 & 0 & 0 & 0 & 0 & 0 & 0 & 0 & 0 & 0 & 0 & 0 & 0 & 0 & 1 & 1 & 1 \end{bmatrix}, \tag{S7a}$$

with 0.8 and 0.2 arising because we assume that 80% of 15–19 year-olds are under 18 and 20% are 18 or older, and

$$\mathbf{G}_{\mathrm{H}} = \begin{bmatrix} 1 & 1 & 1 & 1 & 1 & 1 & 1 & 1 & 1 & 1 & 1 & 1 & 1 & 1 & 1 & 1 & 1 \end{bmatrix}, \tag{S7b}$$

since high-risk people of all ages are combined into one vaccination group. Then, given the proportions vaccinated in the vaccination age groups, $p_{\mathbf{L}ra_{\mathrm{L}}}$ and $p_{\mathbf{H}ra_{\mathrm{H}}}$, the quantities

$$q_{\mathrm{L}ra} = \sum_{a_{\mathrm{L}}} G_{\mathrm{L}aa_{\mathrm{L}}} p_{\mathrm{L}ra_{\mathrm{L}}}, \tag{S8a}$$

$$q_{\mathrm{H}ra} = \sum_{a_{\mathrm{H}}} G_{\mathrm{H}aa_{\mathrm{H}}} p_{\mathrm{H}ra_{\mathrm{H}}}, \tag{S8b}$$

are the proportions vaccinated in the model age groups.

We take vaccination to only be done to unvaccinated susceptible people and to instantaneously protect people, so that the state variables change discontinuously at $t = t_r$:

$$S_{\mathrm{LU}a}(t_r^+) = (1 - q_{\mathrm{L}ra}) S_{\mathrm{LU}a}(t_r^-), \tag{S9a}$$

$$S_{\mathrm{HU}a}(t_r^+) = (1 - q_{\mathrm{H}ra}) S_{\mathrm{HU}a}(t_r^-), \tag{S9b}$$

$$S_{\mathrm{LV}a}(t_r^+) = S_{\mathrm{LV}a}(t_r^-) + q_{\mathrm{L}ra} S_{\mathrm{LU}a}(t_r^-), \tag{S9c}$$

$$S_{\mathrm{HV}a}(t_r^+) = S_{\mathrm{HV}a}(t_r^-) + q_{\mathrm{H}ra} S_{\mathrm{HU}a}(t_r^-), \tag{S9d}$$

with the other state variables remaining the same.

The cumulative number of infections at time T is

$$N_{\mathrm{ILU}a}(T) = N_{\mathrm{LU}a}(0) + \sum_r \left[S_{\mathrm{LU}a}(t_r^+) - S_{\mathrm{LU}a}(t_r^-)\right] - S_{\mathrm{LU}a}(T), \tag{S10a}$$

$$N_{\mathrm{IHU}a}(T) = N_{\mathrm{HU}a}(0) + \sum_r \left[S_{\mathrm{HU}a}(t_r^+) - S_{\mathrm{HU}a}(t_r^-)\right] - S_{\mathrm{HU}a}(T), \tag{S10b}$$

$$N_{\mathrm{ILV}a}(T) = N_{\mathrm{LV}a}(0) + \sum_r \left[S_{\mathrm{LV}a}(t_r^+) - S_{\mathrm{LV}a}(t_r^-)\right] - S_{\mathrm{LV}a}(T), \tag{S10c}$$

$$N_{\mathrm{IHV}a}(T) = N_{\mathrm{HV}a}(0) + \sum_r \left[S_{\mathrm{HV}a}(t_r^+) - S_{\mathrm{HV}a}(t_r^-)\right] - S_{\mathrm{HV}a}(T), \tag{S10d}$$

for unvaccinated low-risk, unvaccinated high-risk, vaccinated low-risk, and vaccinated high-risk people, respectively. The middle terms in equations (S10), those with the summations, account for the change in vaccination status when vaccine is distributed. Here

$$N_{\mathrm{LU}a} = S_{\mathrm{LU}a} + E_{\mathrm{LU}a} + I_{\mathrm{LU}a} + R_{\mathrm{LU}a}, \tag{S11a}$$

$$N_{\mathrm{HU}a} = S_{\mathrm{HU}a} + E_{\mathrm{HU}a} + I_{\mathrm{HU}a} + R_{\mathrm{HU}a}, \tag{S11b}$$

$$N_{\mathrm{LV}a} = S_{\mathrm{LV}a} + E_{\mathrm{LV}a} + I_{\mathrm{LV}a} + R_{\mathrm{LV}a}, \tag{S11c}$$

$$N_{\mathrm{HV}a} = S_{\mathrm{HV}a} + E_{\mathrm{HV}a} + I_{\mathrm{HV}a} + R_{\mathrm{HV}a}, \tag{S11d}$$

are the numbers of people summed over infection status. The cumulative number of deaths is

$$N_{\mathrm{D}a}(T) = N_a(0) - N_a(T), \tag{S12}$$

where N_a is the total number of people in age group a

$$N_a = N_{\mathrm{LU}a} + N_{\mathrm{HU}a} + N_{\mathrm{LV}a} + N_{\mathrm{HV}a}. \tag{S13}$$

We will minimize, at the end time T, the objective function that is either total deaths

$$D(T) = \sum_a N_{\mathrm{D}a}(T) \tag{S14}$$

or total hospitalizations

$$H(T) = \sum_a \left[c_{\mathrm{L}a} N_{\mathrm{IL}a}(T) + c_{\mathrm{H}a} N_{\mathrm{IH}a}(T)\right], \tag{S15}$$

where

$$N_{\mathrm{IL}a} = N_{\mathrm{ILU}a} + N_{\mathrm{ILV}a}, \tag{S16a}$$

$$N_{\mathrm{IH}a} = N_{\mathrm{IHU}a} + N_{\mathrm{IHV}a}, \tag{S16b}$$

are the numbers of infections in age group a to low-risk and high-risk people, respectively, and $c_{\mathrm{L}a}$ and $c_{\mathrm{H}a}$ are the case hospitalizations for low-risk and high-risk people in age group a. Note that here we have assumed that the risk of hospitalization is independent of vaccination status.

The problem is, given the starting time (t_0), the end time (T) and the vaccine delivery schedule ($t_1, t_2, \ldots, t_R$ and $v_1, v_2, \ldots, t_R$), find the $p_{\mathrm{L}ra_{\mathrm{L}}}$ and $p_{\mathrm{H}ra_{\mathrm{H}}}$ that minimize objective function (S14) or (S15), subject to the feasibility conditions

$$0 \leq p_{\mathrm{L}ra_{\mathrm{L}}} \leq 1, \tag{S17a}$$

$$0 \leq p_{\mathrm{H}ra_{\mathrm{H}}} \leq 1, \tag{S17b}$$

$$\sum_a \left[q_{\mathrm{L}ra} S_{\mathrm{LU}a} + q_{\mathrm{H}ra} S_{\mathrm{HU}a}\right] \leq v_r, \tag{S17c}$$

the latter of which ensures that the number of vaccines used is below the number available; the initial conditions (S2) at $t = t_0$; the differential equations (S1) on $t_k < t \leq t_{k+1}$ for $k = 0, 1, 2, \ldots, R$, where $t_{R+1} = T$; and the jump conditions (S9) at $t = t_r$ for $r = 1, 2, \ldots R$.

For a given vaccine distribution schedule, the optimal vaccine allocations were found numerically using the constrained optimization by linear approximation (COBYLA) algorithm [12], run 3 times with random initial vaccination levels. We took the optimum to be the result with the smallest value of the objective function among these 3 runs.

S2 Parameter Values

The model epidemiological parameters are listed in Table S2. The latent period, the time between becoming infected and becoming infectious, has not been estimated directly, but the incubation period, the time between becoming infected and becoming symptomatic, has [10, 15]. We assumed that a person becomes infections 1 day before becoming symptomatic [10], so that the latent period is 1 day shorter than the incubation period. Analysis of the first 11 cases of 2009 H1N1 documented by the U.S. Centers for Disease Control and Prevention found a median incubation period of 3 days [15]. The infectious period is not known for 2009 H1N1, so we have taken it to be 7 days as the upper end of the range from seasonal influenzas [10].

In addition, we parametrized the contact matrix ($\phi_{a\alpha}$), which describes the number of potentially transmitting contacts per day between a person in

Table S2: Epidemiological parameter values.

Parameter	**Ages**	**Value**	**Reference**
Latent period, $1/\tau$	all	2 d	[10, 15]
Infectious period, $1/\gamma$	all	7 d	[10]
Relative susceptibility, σ_a	0–4	1	[8]
	5–24	0.98	
	25–49	0.94	
	50–64	0.91	
	65+	0.66	
Vaccine efficacy against infection, ϵ_a	$<$ 6 m	0	[1]
	6 m–64	0.75	
	65+	0.5	
Vaccine efficacy against death, δ_a	0–19	0.75	[7]
	20–64	0.7	
	65+	0.6	
Case mortality (per 1000 cases), d_a	0–4	0.22	[13]
	5–17	0.09	
	18–64	1.36	
	65+	0.28	
Case hospitalization (per 1000 cases) c_a	0–4	21.9	[13]
	5–17	5.3	
	18–64	26.6	
	65+	5.7	

age group a and people in age group α, as in Medlock and Galvani [6], using survey-based data [9].

In our model, the only impact of being in the high-risk group was an increased risk of averse outcomes, death and hospitalization, from influenza infection. We assumed that high-risk people are 9 times more likely to die from an infection and 3 times more likely to be hospitalized. These risk ratios are consistent with those found for seasonal influenzas [see 7, and references therein].

We assumed that the empirical case mortality (d_a, Table S2) was to people with the same proportion of the risk groups as the overall population (Table S1) and, of course, to all unvaccinated people. The case mortality for

low-risk, unvaccinated people is then

$$d_{\mathrm{LU}a} = \frac{d_a}{(1 - P_{\mathrm{H}a}) + 9P_{\mathrm{H}a}}. \tag{S18}$$

Then the case mortality in terms of the model parameters recovery rate (γ) and death rate for low-risk, unvaccinated people ($\nu_{\mathrm{LU}a}$), is

$$d_{\mathrm{LU}a} = \frac{\nu_{\mathrm{LU}a}}{\gamma + \nu_{\mathrm{LU}a}}. \tag{S19}$$

Therefore,

$$\nu_{\mathrm{LU}a} = \gamma \frac{d_{\mathrm{LU}a}}{1 - d_{\mathrm{LU}a}}. \tag{S20a}$$

This is the death rate for low-risk, unvaccinated people. The case mortality for low-risk, vaccinated people is then reduced by the vaccine efficacy against death (δ_a), giving

$$\nu_{\mathrm{LV}a} = \gamma \frac{(1 - \delta_a) d_{\mathrm{LU}a}}{1 - (1 - \delta_a) d_{\mathrm{LU}a}}. \tag{S20b}$$

We assume high-risk people have a 9 times higher risk of death (Table S3), so that the death rates are

$$\nu_{\mathrm{HU}a} = \gamma \frac{9 d_{\mathrm{HU}a}}{1 - 9 d_{\mathrm{HU}a}}, \tag{S20c}$$

$$\nu_{\mathrm{HV}a} = \gamma \frac{9(1 - \delta_a) d_{\mathrm{HU}a}}{1 - 9(1 - \delta_a) d_{\mathrm{HU}a}}. \tag{S20d}$$

Note here that we have assumed that the vaccine efficacy against death reduces the case mortality by the same relative amount in both low-risk and high-risk people.

Similarly, we took the empirical case hospitalization (c_a) to be to people in the same proportion of the risk groups as the overall population. Then the model case hospitalization for low-risk people ($c_{\mathrm{L}a}$) is

$$c_{\mathrm{L}a} = \frac{c_a}{(1 - P_{\mathrm{H}a}) + 3P_{\mathrm{H}a}}. \tag{S21}$$

and the case hospitalization for high-risk people to be 3 times higher (Table S3), $c_{\mathrm{H}a} = 3c_{\mathrm{L}a}$.

The one remaining parameter, the probability of transmission given a suitable contact (β), was then chosen so that the model's basic reproductive number (in the absence of vaccination) had a proscribed value. We considered $R_0 = 1.2$, 1.4, 1.7, and 2.0.

Table S3: Relative risk of averse outcomes for high-risk people versus low-risk people.

Outcome	Relative Risk
Death	9
Hospitalization	3

From Meltzer et al. [7]. See text for more.

S3 Results

Figure S1 shows epidemic curves for different age groups for an outbreak with $R_0 = 1.4$ and no vaccination. The transmission model has 17 age groups: the 17 age groups were combined into just 5 age groups to simplify the figure.

To simulate the ongoing 2009 H1N1 influenza pandemic, we took the estimate of 1 million cumulative cases on 1 August 2009 [14] and the vaccine delivery schedule as 45 million doses on 15 October 2009 and 20 million doses each week thereafter. We compared vaccine delivery schedules with only the first batch of 45 million doses; with two batches, a 45 million dose batch and then a 20 million dose batch; with three batches, 45 million dose batch and then two 20 million dose batches; and so on, up to a 45 million dose batch followed by eight 20 million dose batches. In addition, we also compared two more delivery schedules, a single batch of 125 million doses on 15 October and a single batch of 125 million doses before the outbreak began. For each of these vaccine delivery schedules, we found the optimal age- and risk-dependent allocation that minimized either deaths or hospitalizations (Figures 1, 2, & S2–S15).

Figures S8–S15 show the optimal allocations of multiple batches of vaccine for a given number of batches. Of particular interest is that the optimal allocations for multiple batches cannot be found by iteratively finding the optimal allocation for the first batch, then for the second batch given the allocation for the first batch, and so on. The optimal allocation in each batch depends on the total number of batches. For example, for $R_0 = 1.2$ and deaths averted (Figure S8), the optimal allocation when there are 2 total batches of vaccine includes vaccinating some 18–44 year olds in the second batch, while, when there are 3 total batches of vaccine, vaccinating 18–44 year olds is not optimal.

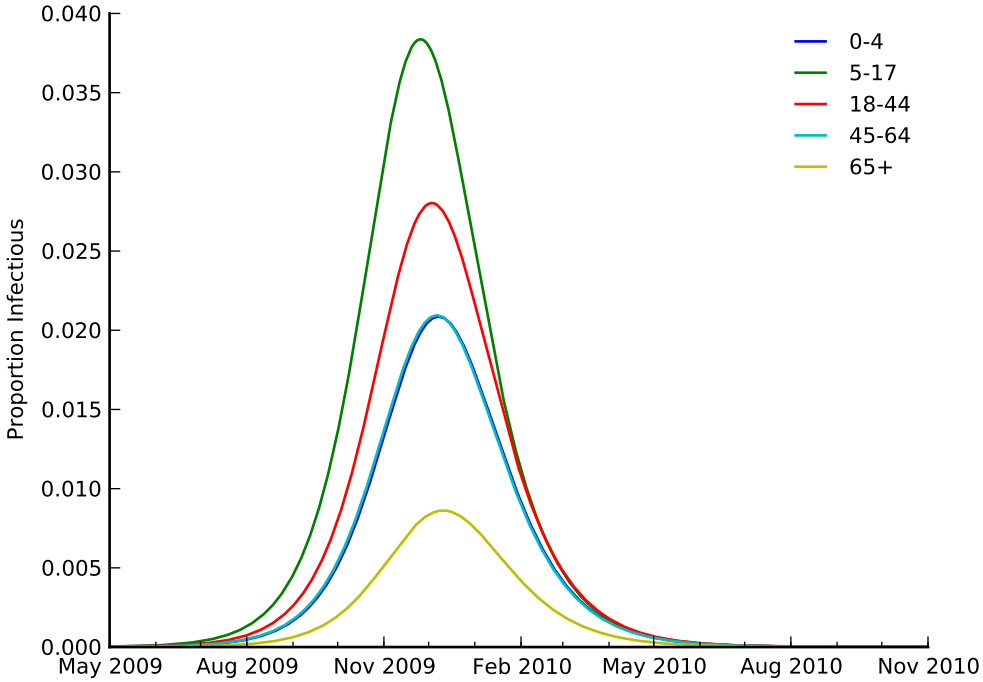

Figure S1: Model epidemic curves for different age groups with $R_0 = 1.4$ and no vaccination.

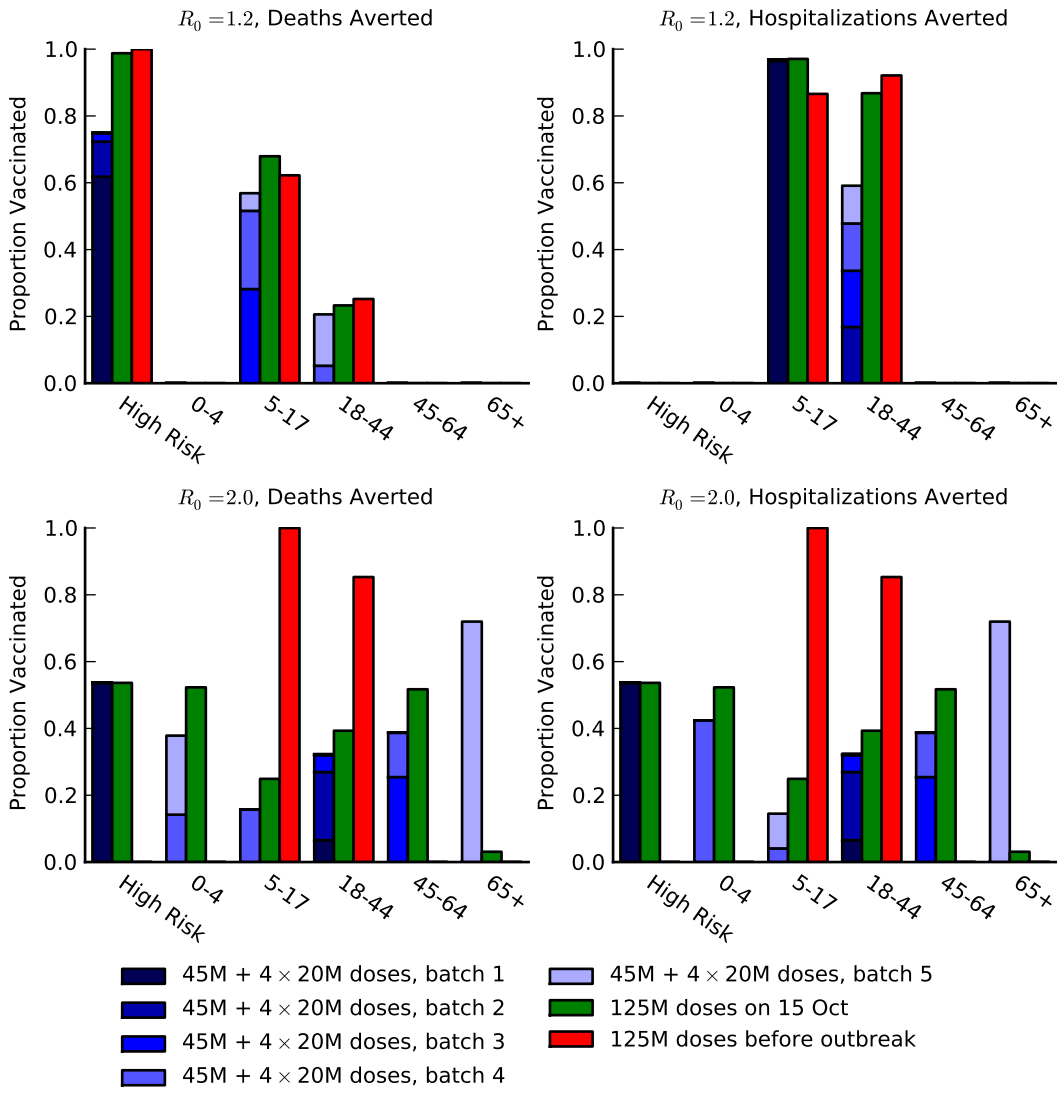

Figure S2: Optimal vaccine allocation for different vaccine delivery schedules, different values of R_0, and different objectives. The delivery schedule "45M + 4 ×20M doses" corresponds to 5 batches of vaccine delivery: 45M doses on 15 October and 20M doses each of the following 4 weeks. The different shades of blue correspond to the optimal allocation of the different delivery batches: i.e. the darkest blue describes the optimal allocation for the first 45M doses, the next darkest shade describes the allocation for the 20M doses delivered the following week, and so on. The graphs for $R_0 = 1.4$ and 1.7 are in the main text.

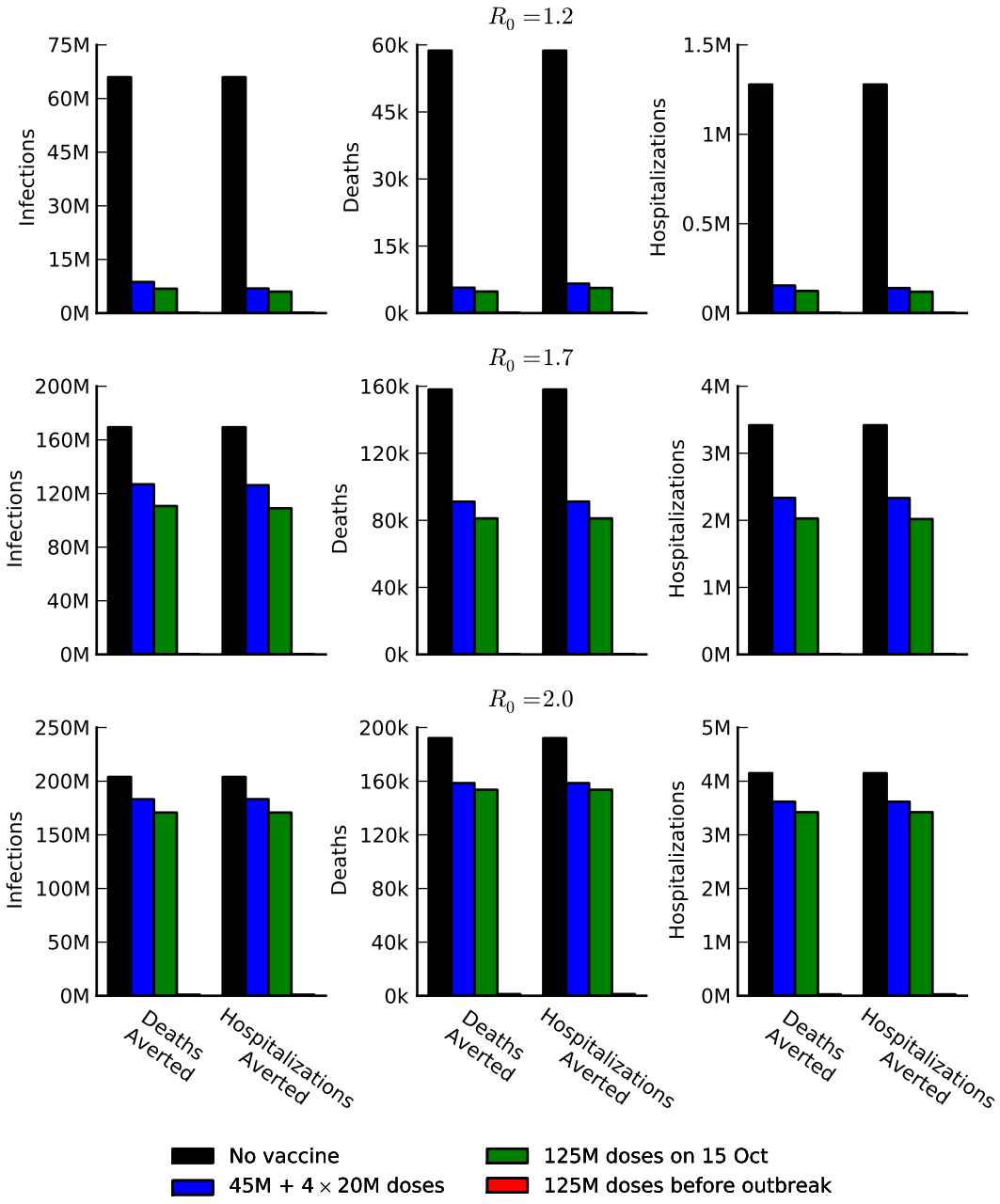

Figure S3: The impact on infections, deaths, and hospitalizations for different vaccine delivery schedules, different values of R_0, and different objectives. The graphs for $R_0 = 1.4$ are in the main text.

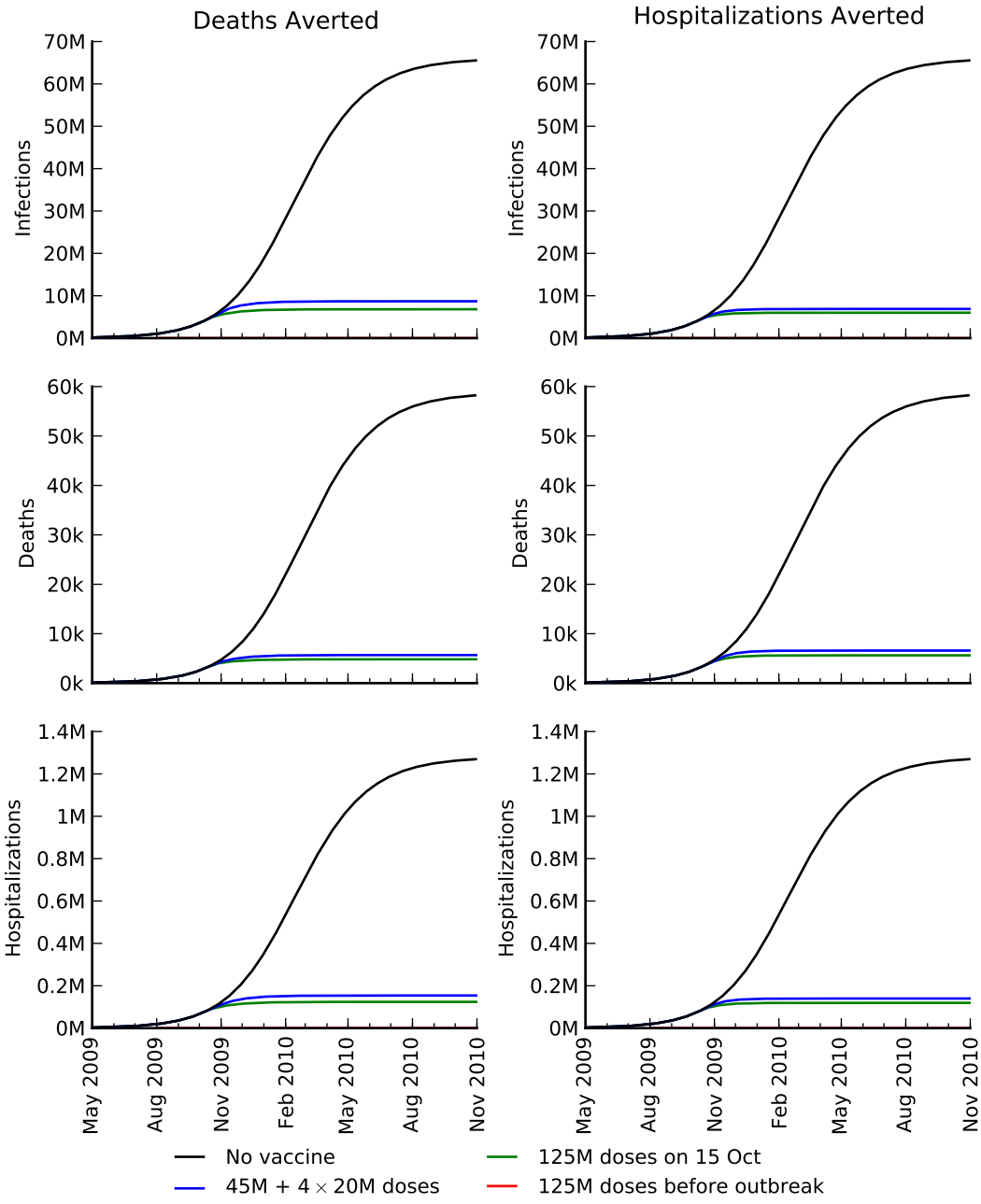

Figure S4: The time course of cumulative infections, deaths, and hospitalizations for different vaccine delivery schedules and different objectives with $R_0 = 1.2$.

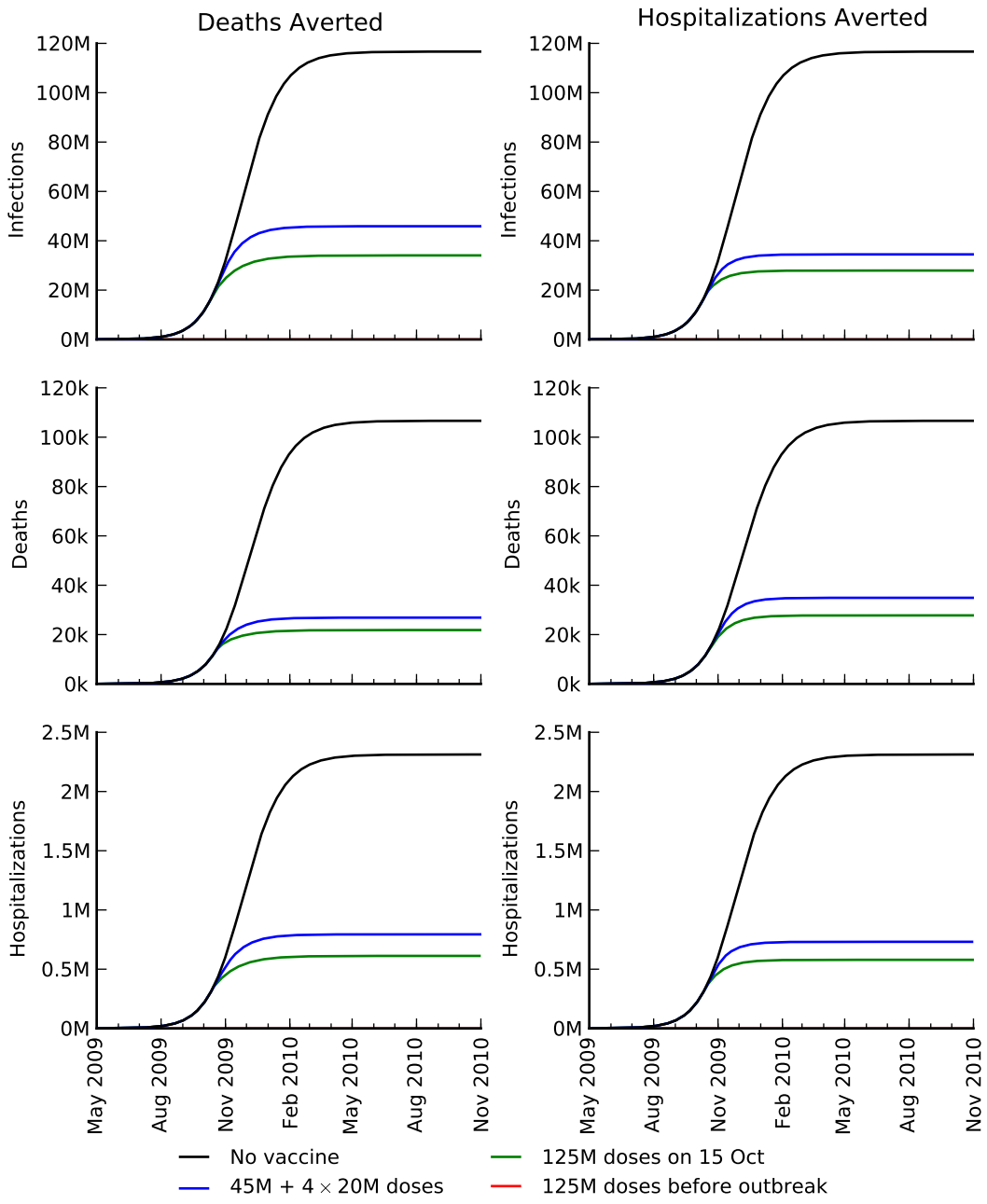

Figure S5: The time course of cumulative infections, deaths, and hospitalizations for different vaccine delivery schedules and different objectives with $R_0 = 1.4$.

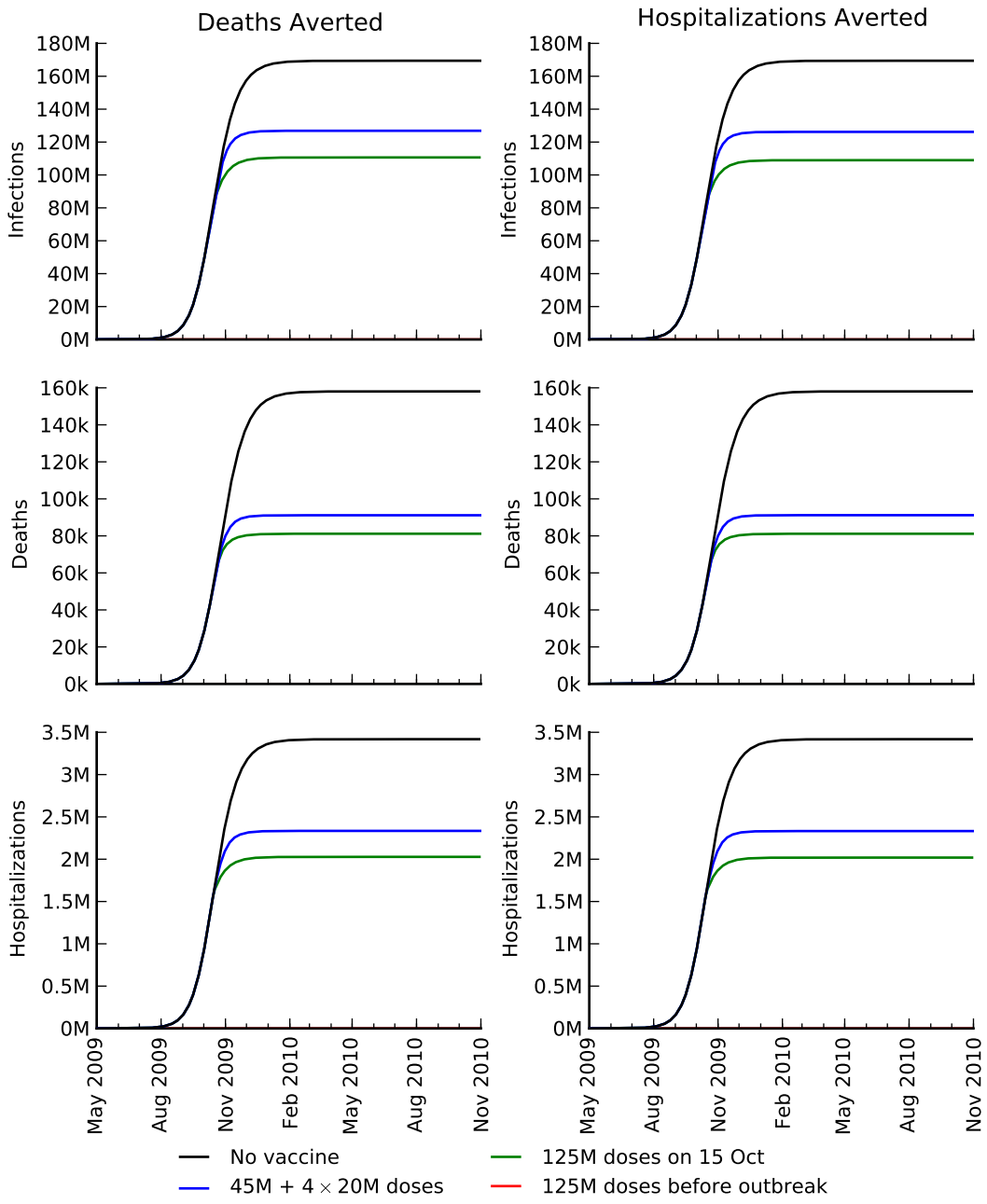

Figure S6: The time course of cumulative infections, deaths, and hospitalizations for different vaccine delivery schedules and different objectives with $R_0 = 1.7$.

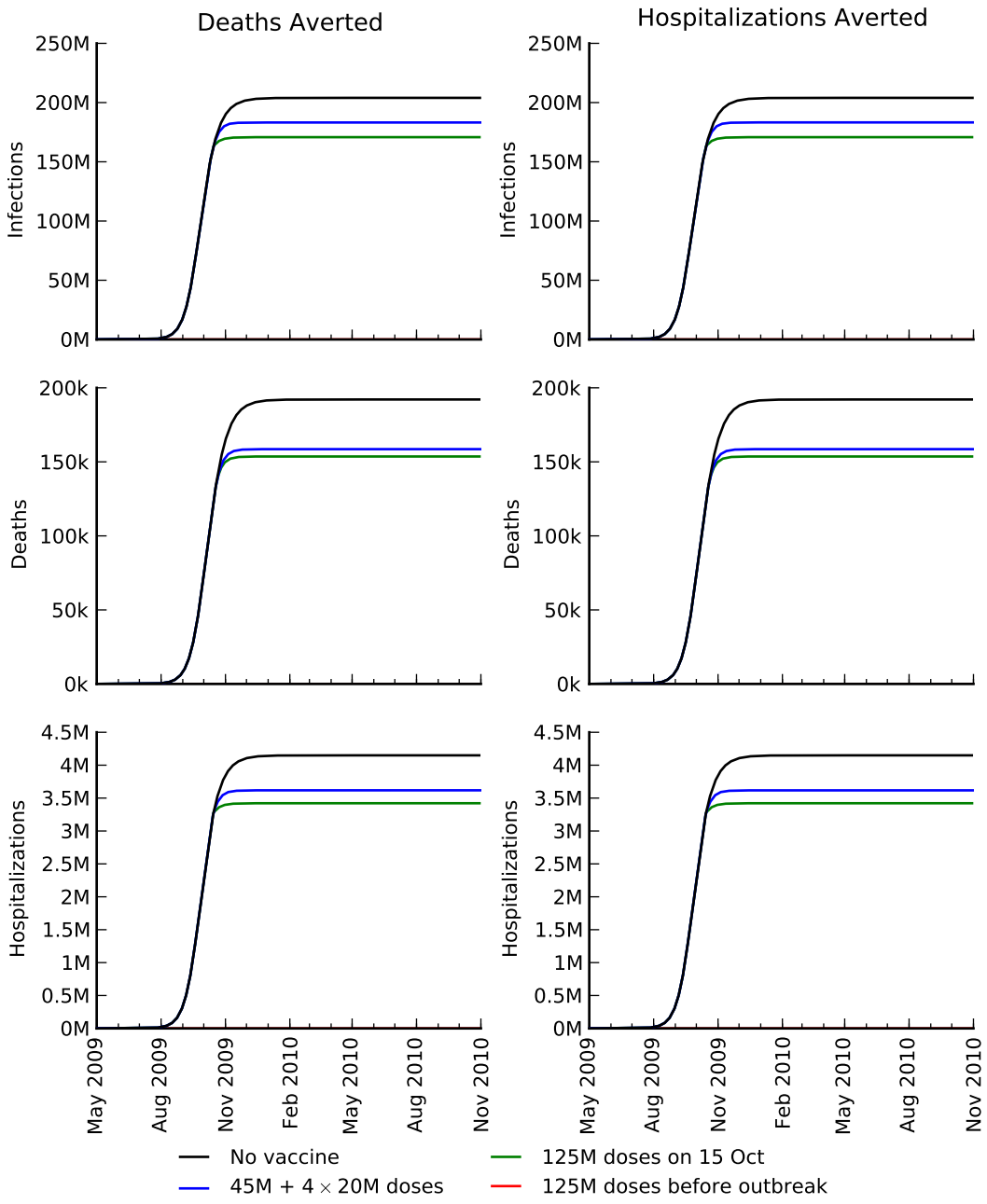

Figure S7: The time course of cumulative infections, deaths, and hospitalizations for different vaccine delivery schedules and different objectives with $R_0 = 2.0$.

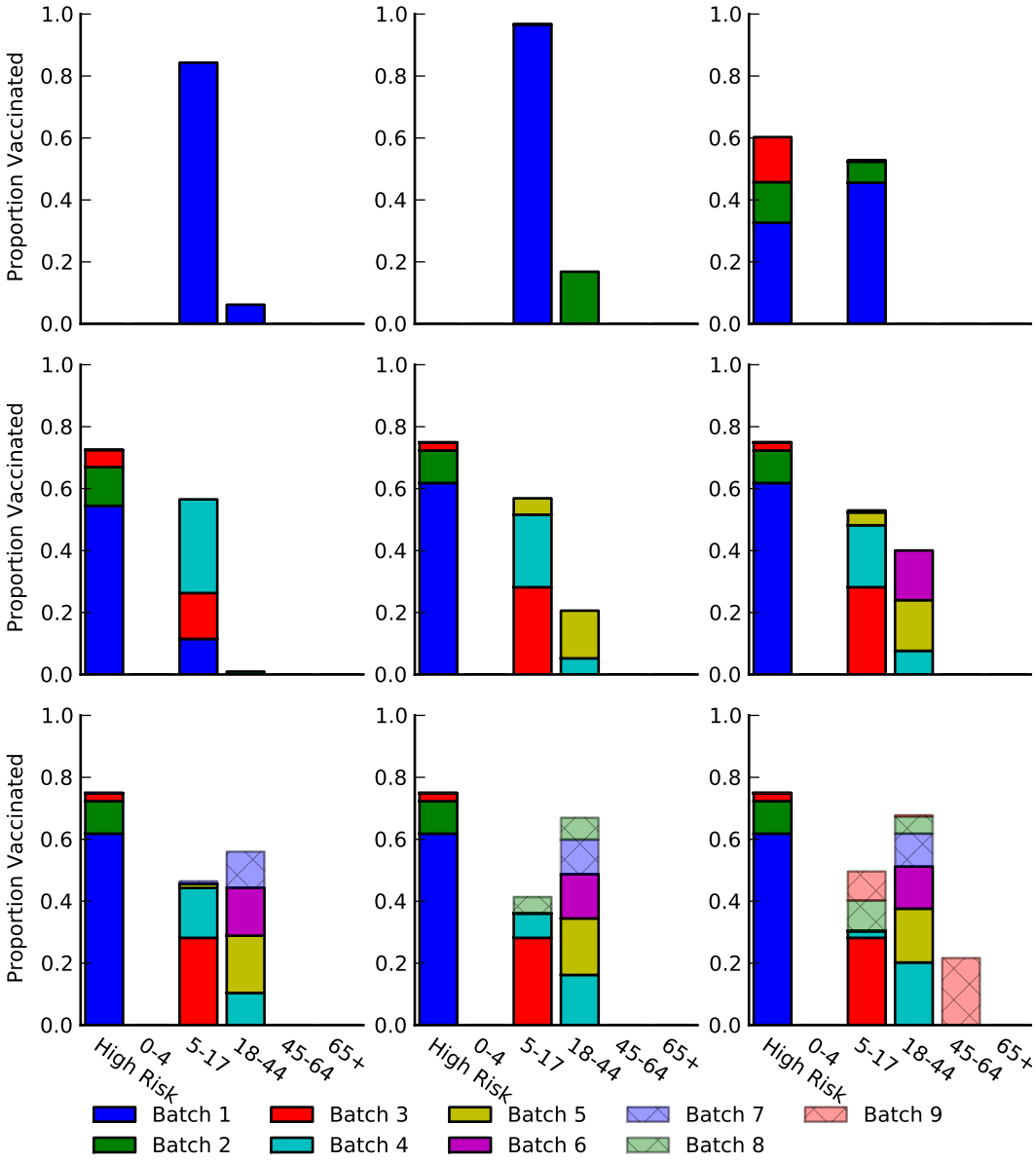

Figure S8: Optimal vaccine allocation for different numbers of vaccine batches for $R_0 = 1.2$ and deaths averted. The delivery schedules consist of from 1 to 8 batches of vaccine delivered in intervals of 1 week, with the first batch being 45M doses and subsequent batches being 20M doses. Each graph shows the optimal allocation given the number of batches of vaccine available.

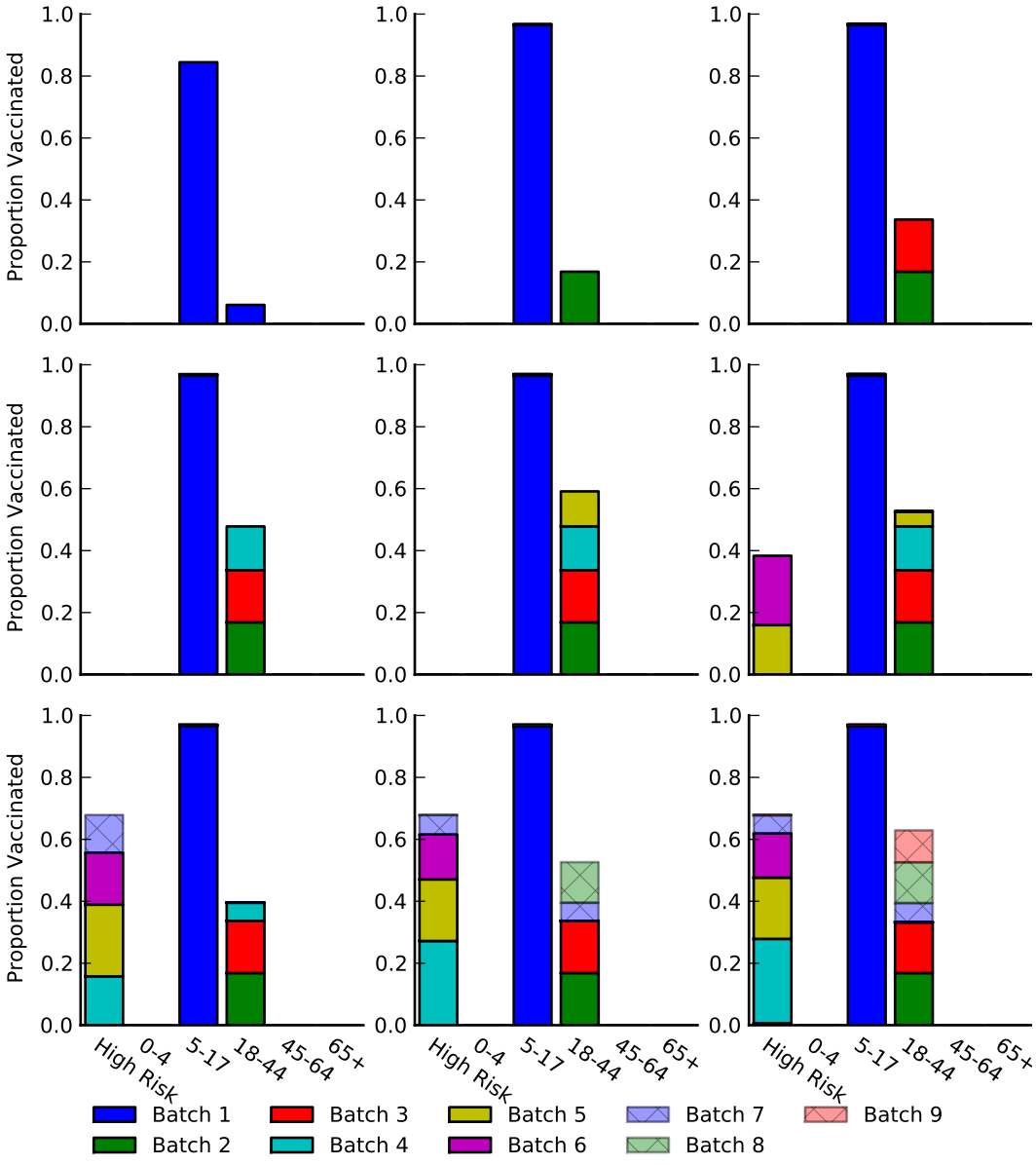

Figure S9: Optimal vaccine allocation for different numbers of vaccine batches for $R_0 = 1.2$ and hospitalizations averted. The delivery schedules consist of from 1 to 8 batches of vaccine delivered in intervals of 1 week, with the first batch being 45M doses and subsequent batches being 20M doses. Each graph shows the optimal allocation given the number of batches of vaccine available.

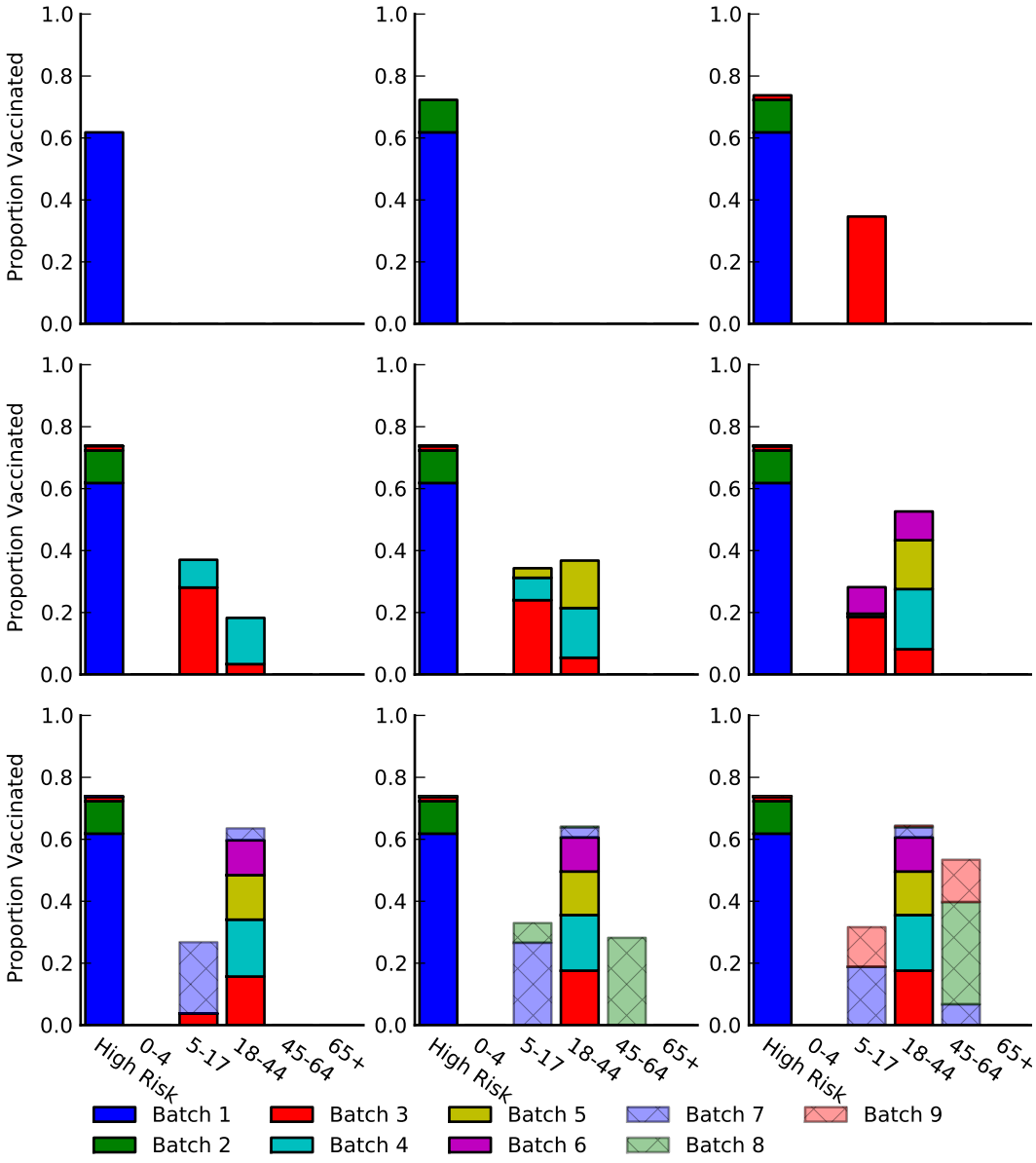

Figure S10: Optimal vaccine allocation for different numbers of vaccine batches for $R_0 = 1.4$ and deaths averted. The delivery schedules consist of from 1 to 8 batches of vaccine delivered in intervals of 1 week, with the first batch being 45M doses and subsequent batches being 20M doses. Each graph shows the optimal allocation given the number of batches of vaccine available.

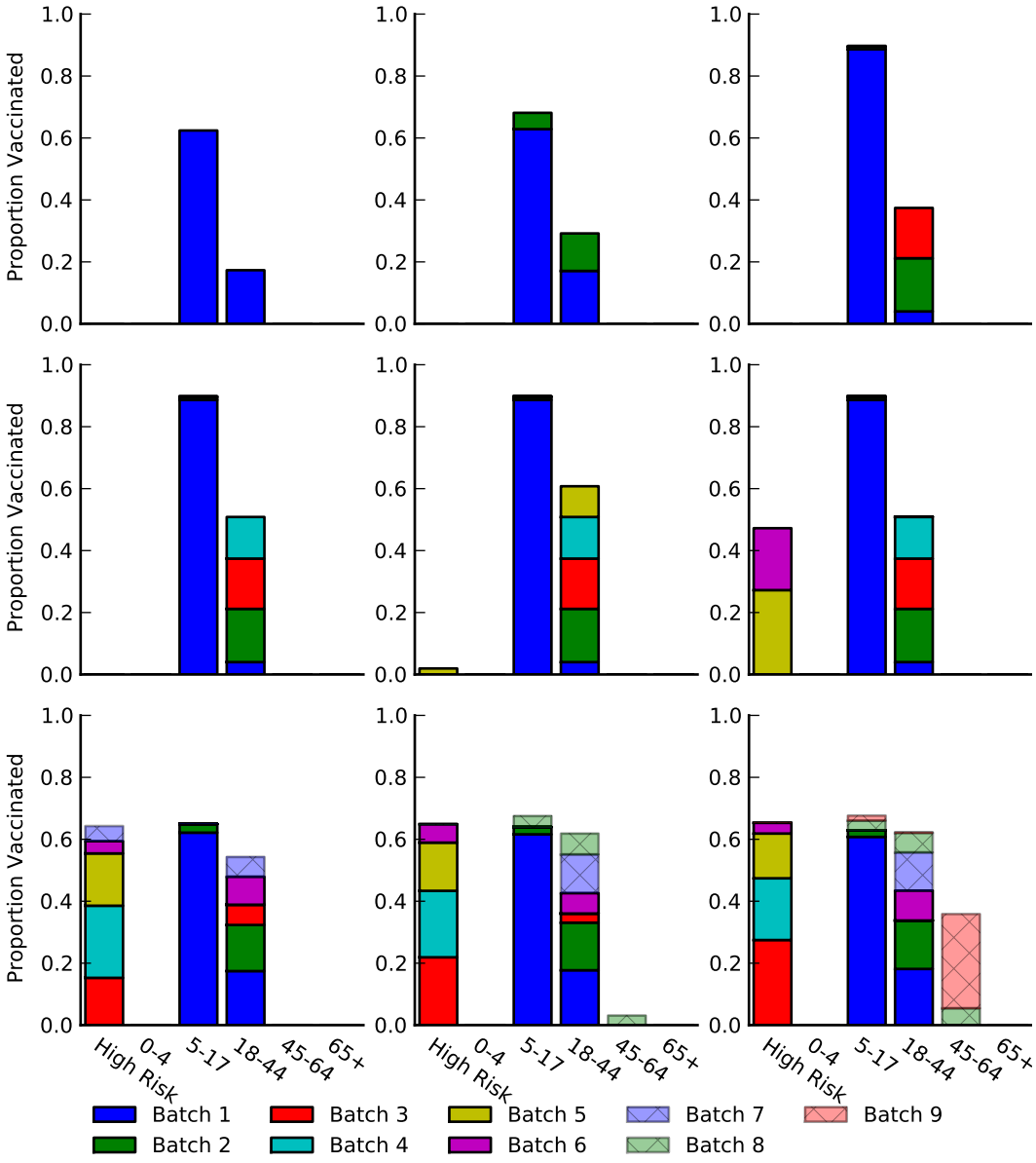

Figure S11: Optimal vaccine allocation for different numbers of vaccine batches for $R_0 = 1.4$ and hospitalizations averted. The delivery schedules consist of from 1 to 8 batches of vaccine delivered in intervals of 1 week, with the first batch being 45M doses and subsequent batches being 20M doses. Each graph shows the optimal allocation given the number of batches of vaccine available.

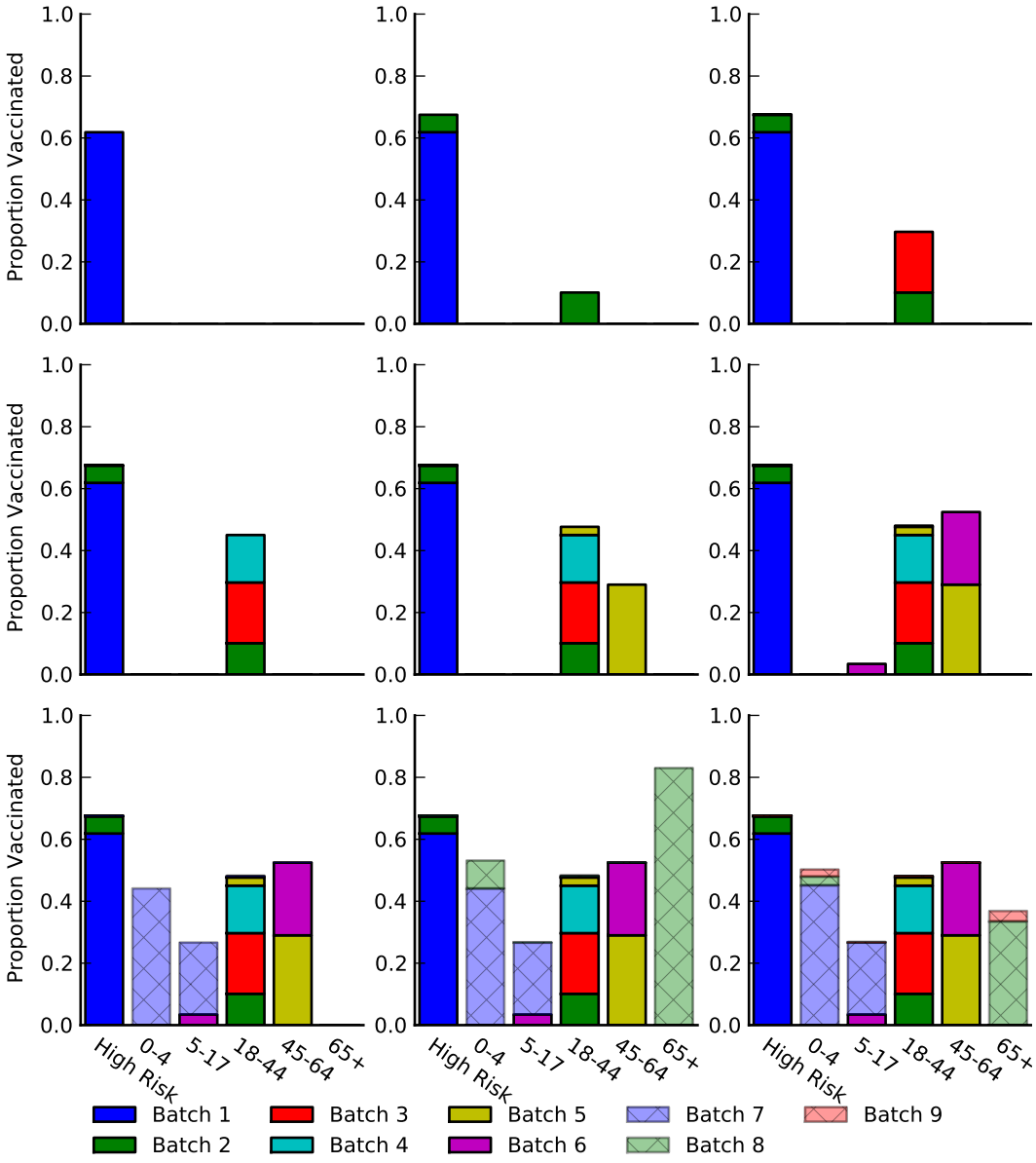

Figure S12: Optimal vaccine allocation for different numbers of vaccine batches for $R_0 = 1.7$ and deaths averted. The delivery schedules consist of from 1 to 8 batches of vaccine delivered in intervals of 1 week, with the first batch being 45M doses and subsequent batches being 20M doses. Each graph shows the optimal allocation given the number of batches of vaccine available.

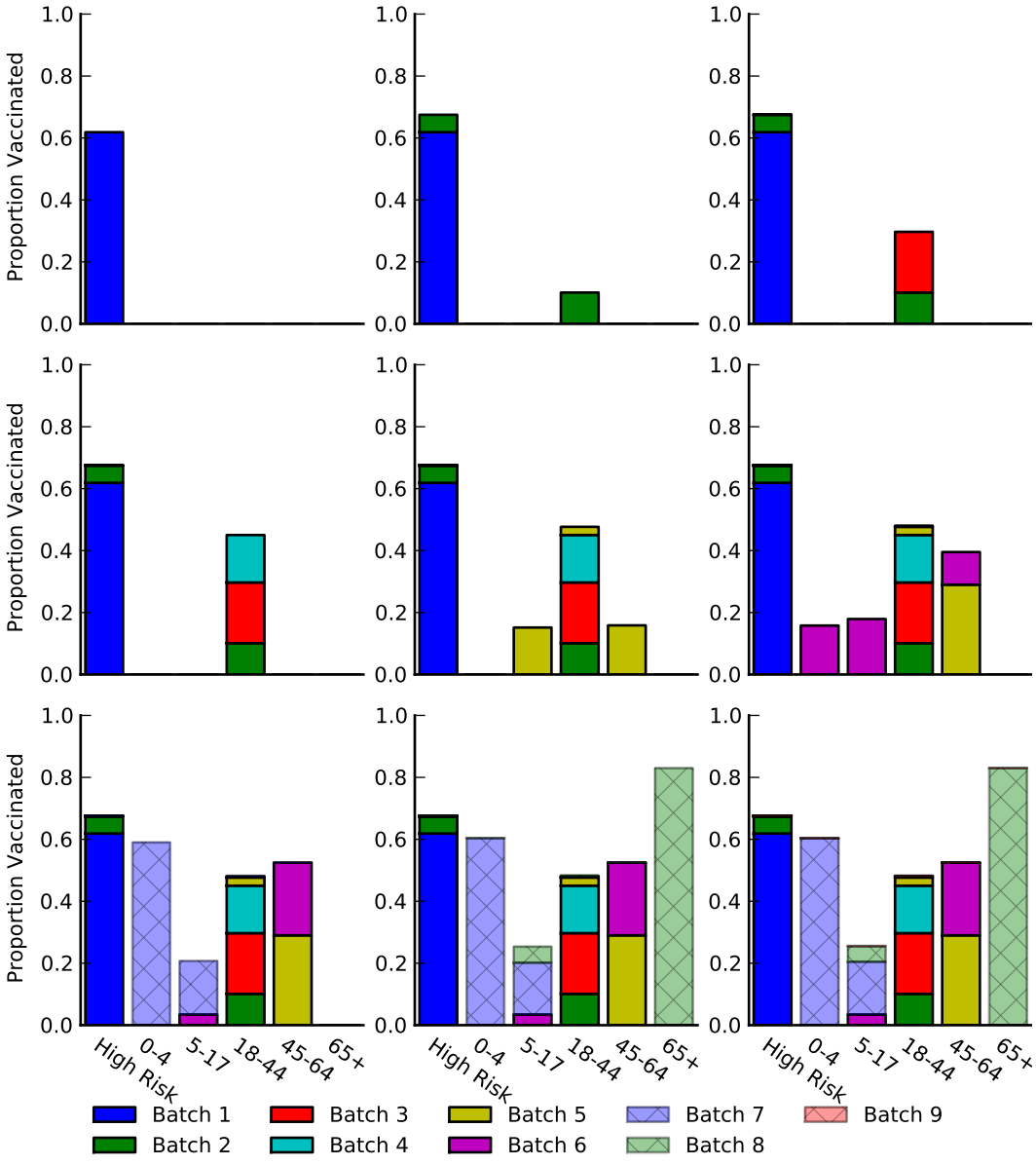

Figure S13: Optimal vaccine allocation for different numbers of vaccine batches for $R_0 = 1.7$ and hospitalizations averted. The delivery schedules consist of from 1 to 8 batches of vaccine delivered in intervals of 1 week, with the first batch being 45M doses and subsequent batches being 20M doses. Each graph shows the optimal allocation given the number of batches of vaccine available.

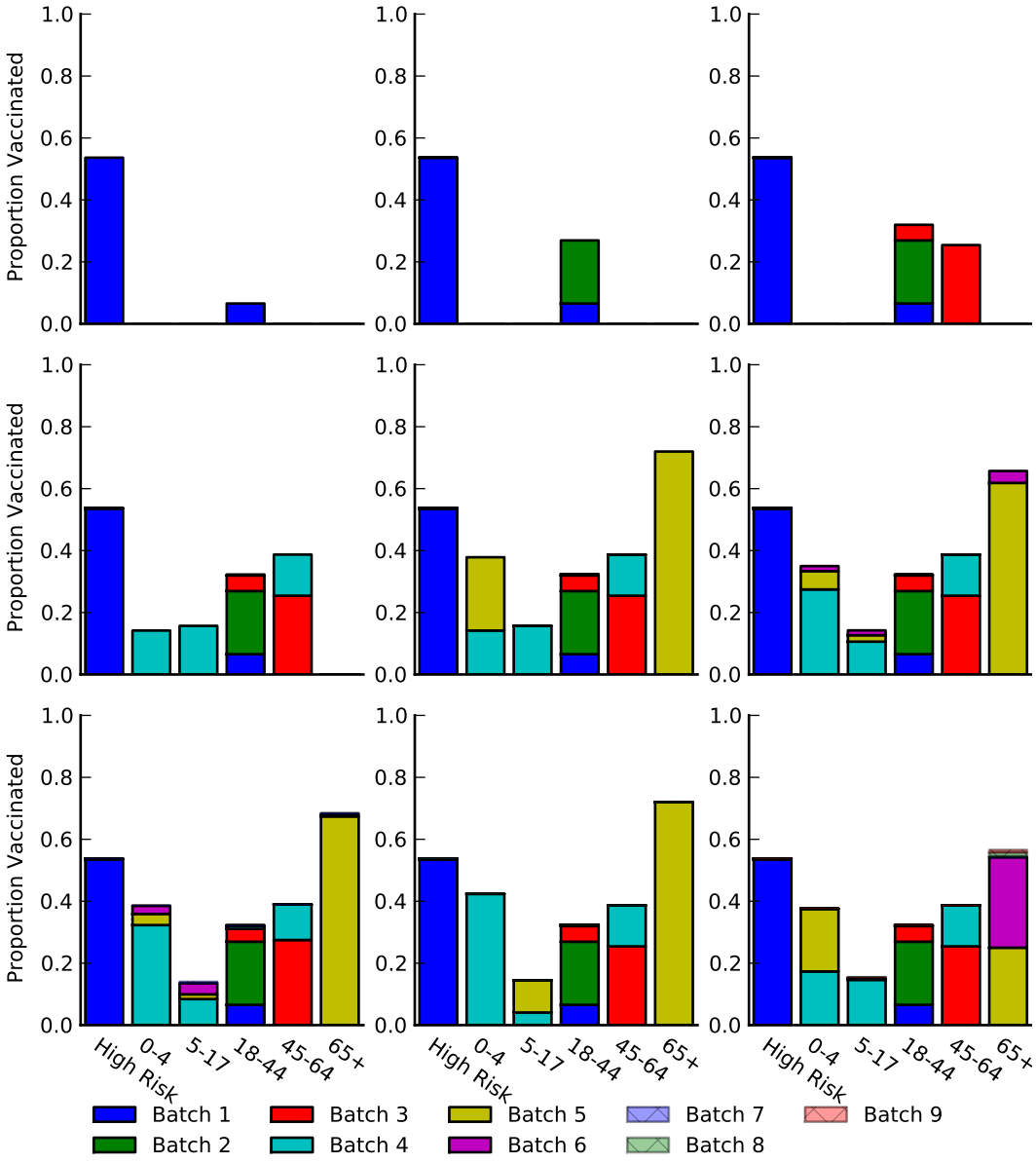

Figure S14: Optimal vaccine allocation for different numbers of vaccine batches for $R_0 = 2.0$ and deaths averted. The delivery schedules consist of from 1 to 8 batches of vaccine delivered in intervals of 1 week, with the first batch being 45M doses and subsequent batches being 20M doses. Each graph shows the optimal allocation given the number of batches of vaccine available.

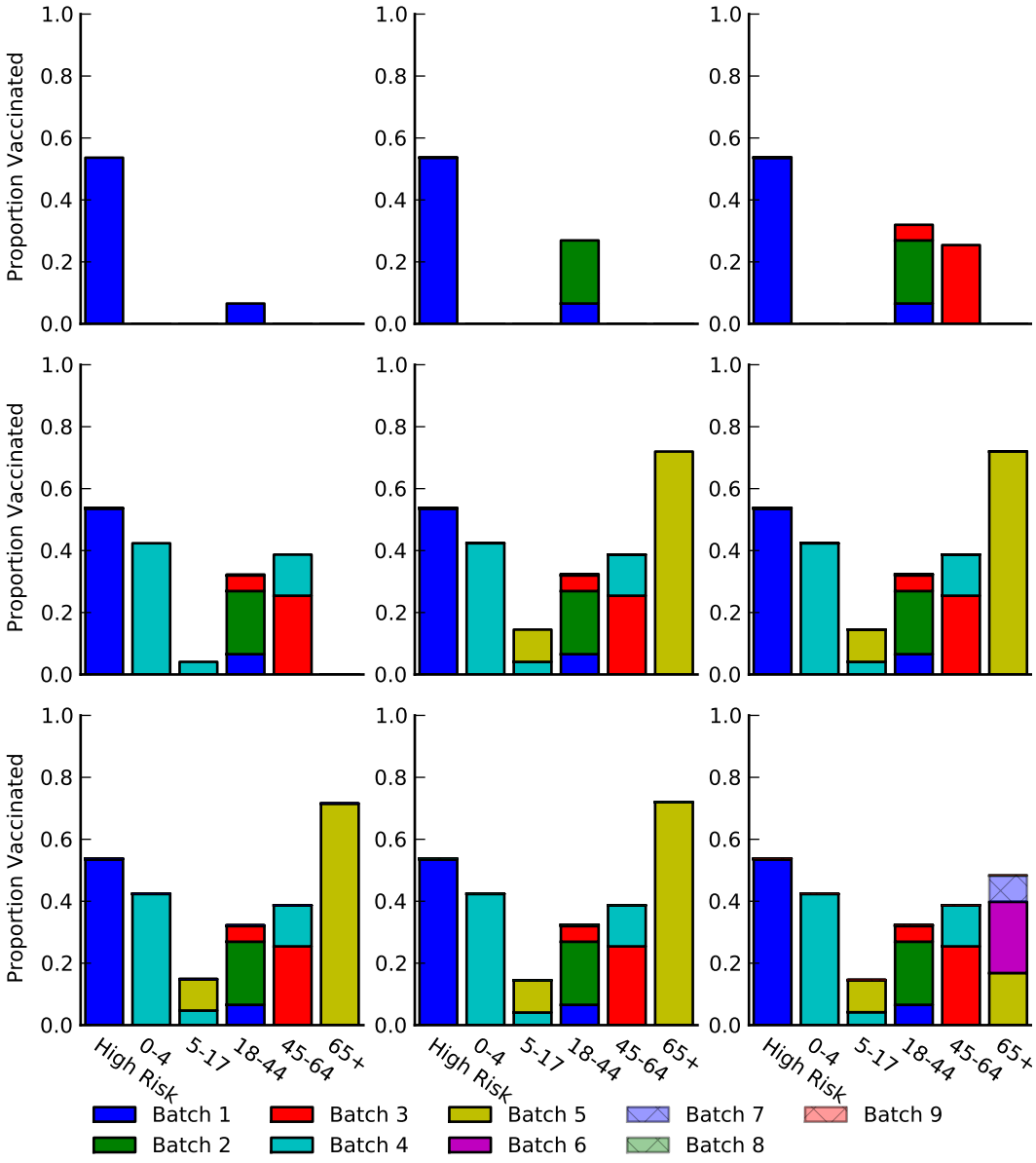

Figure S15: Optimal vaccine allocation for different numbers of vaccine batches for $R_0 = 2.0$ and hospitalizations averted. The delivery schedules consist of from 1 to 8 batches of vaccine delivered in intervals of 1 week, with the first batch being 45M doses and subsequent batches being 20M doses. Each graph shows the optimal allocation given the number of batches of vaccine available.

References

[1] N. E. Basta, M. E. Halloran, L. Matrajt, and I. M. Longini Jr. Estimating influenza vaccine efficacy from challenge and community-based study data. *Am J Epidemiol*, 170(6):679–686, 2008.

[2] Centers for Disease Control and Prevention. *National Health Interview Survey*, 2006–2008. URL `http://www.cdc.gov/NCHS/nhis/`.

[3] Centers for Disease Control and Prevention. *HIV/AIDS Surveillance Report*, 2007. URL `http://www.cdc.gov/hiv/topics/surveillance/resources/reports/2007report/default.htm`.

[4] O. Diekmann, J. Heesterbeek, and J. Metz. On the definition and the computation of the basic reproduction ratio r_0 in models for infectious diseases in heterogeneous populations. *J Math Biol*, 28(4):365–382, 1990. ISSN 0303-6812.

[5] A. C. Hindmarsh. *Brief Description of ODEPACK - A Systematized Collection of ODE Solvers Double Precision Version*, Accessed 12 June 2008. URL `http://www.netlib.org/odepack/opkd-sum`.

[6] J. Medlock and A. P. Galvani. Optimizing influenza vaccine distribution. *Science*, 325(5948):1705–1708, 2009.

[7] M. I. Meltzer, N. J. Cox, and K. Fukuda. Modeling the economic impact of pandemic influenza in the United States: implications for setting priorities for intervention: background paper. Tech. rep., Centers for Disese Control and Prevention, 1999. URL `http://www.cdc.gov/ncidod/EID/vol5no5/meltzerback.htm`. Accessed 28 July, 2007.

[8] MIDAS High-Risk Segmentation Group. H1N1 modeling parameters with high risk data. Personal communication (Diane Wagener), 2009.

[9] J. Mossong, N. Hens, M. Jit, P. Beutels, K. Auranen, R. Mikolajczyk, M. Massari, S. Salmaso, G. S. Tomba, J. Wallinga, J. Heijne, M. Sadkowska-Todys, M. Rosinska, and W. J. Edmunds. Social contacts and mixing patterns relevant to the spread of infectious diseases. *PLoS Med*, 5(3):e74, 2008. `doi:10.1371/journal.pmed.0050074`.

[10] Novel Swine-Origin Influenza A (H1N1) Virus Investigation Team. Emergence of a novel swine-origin influenza A (H1N1) virus in humans. *N Engl J Med*, 360(25):2605, 2009.

[11] Organ Procurement and Transplantation Network. 2009. URL `http://optn.transplant.hrsa.gov/`.

[12] M. J. D. Powell. A direct search optimization method that models the objective and constraint function by linear interpolation. Numerical Analyses Report DAMTP 1992/NA5, University of Cambridge, 1992.

[13] A. M. Presanis, M. Lipsitch, D. De Angelis, New York City Department of Health and Mental Hygiene, The Swine Flu Infestigation Team, A. Hagy, C. Reed, S. Riley, B. Cooper, P. Biedrzycki, and L. Finelli. The severity of pandemic H1N1 influenza in the United States, April–July 2009. *PLoS Curr Influenza*, RRN1042, Accessed 20 October, 2009. URL `http://knol.google.com/k/anne-m-presanis/the-severity-of-pandemic-h1n1-influenza/agr0htar1u6r/16?collectionId=28qm4w0q65e4w.1&position=6#`.

[14] President's Council of Advisors on Science and Technology. *Report to the President on U.S. preparations for 2009-H1N1 influenza*, Accessed October 20, 2009. URL `http://www.whitehouse.gov/assets/documents/PCAST_H1N1_Report.pdf`.

[15] V. Shinde, C. B. Bridges, T. M. Uyeki, B. Shu, A. Balish, X. Xu, S. Lindstrom, L. V. Gubareva, V. Deyde, R. J. Garten, M. Harris, S. Gerber, S. Vagasky, F. Smith, N. Pascoe, K. Martin, D. Dufficy, K. Ritger, C. Conover, P. Quinlisk, A. Klimov, J. S. Bresee, and L. Finelli. Triple-reassortant swine influenza A (H1) in humans in the United States, 2005–2009. *N Engl J Med*, 360(25):2616–2125, 2009.

[16] United States Renal Data System. 2009. URL `http://www.usrds.org/`.

[17] U.S. Census Bureau. *Monthly Postcensal Resident Population, 6/1/2007*, Accessed June 29, 2007. URL `http://www.census.gov/popest/national/asrh/2006_nat_res.html`.

[18] P. van den Driessche and J. Watmough. Reproduction numbers and sub-threshold endemic equilibria for compartmental models of disease transmission. *Math Biosci*, 180:29–48, 2002. ISSN 0025-5564.